Synthesis, Structural Characterization, and Magnetic Properties of Lanthanide Arsolyl Sandwich Complexes

Noah Schwarz,[†] Frederic Krätschmer,[†] Nithin Suryadevara, Sören Schlittenhardt, Mario Ruben, and Peter W. Roesky*

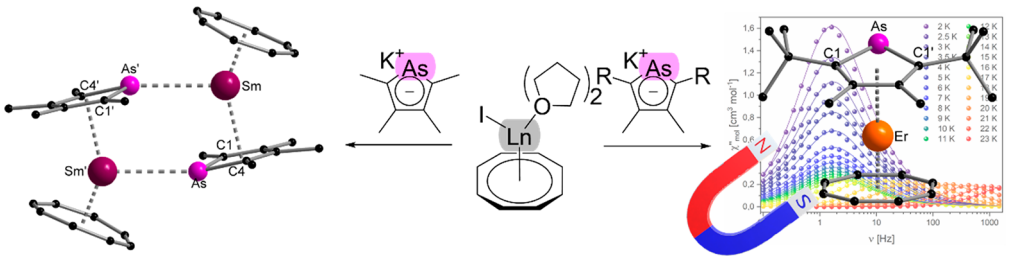

ABSTRACT: A series of trivalent lanthanide sandwich complexes $[(\eta^5\text{-}C_4R_4As)Ln(\eta^8\text{-}C_8H_8)]$ using three different arsolyl ligands are reported. The complexes were obtained via salt elimination reactions between potassium arsolyl salts and lanthanide precursors $[LnI(COT)(THF)_2]$ (Ln = Sm, Dy, Er; COT = η^8-C_8H_8). The resulting compounds exhibit classical sandwich complex structures with one notable exception. Characterization was conducted in both the solid state using single-crystal X-ray diffraction and in solution for the Sm compounds using NMR spectroscopy. Furthermore, the magnetic properties of an Er complex were investigated, revealing distinctive single-molecule-magnet behavior characterized by an energy barrier of U_{eff} = 323.3 K. Theoretical calculations were employed to support and interpret the experimental findings, with a comparative analysis performed against previously reported complexes.

INTRODUCTION

The organometallic chemistry of lanthanides has been dominated by cyclopentadienyl (Cp, $C_5H_5^-$) ligands for a long time. In comparison, the chemistry of heterocyclopentadienyl ligands with rare-earth elements has remained rather underexplored. In 1989, Nief and Mathey reported the first example of a phospholyl complex with Yb and Lu.[1] Later they also succeeded in the isolation of the first lanthanide complex comprising the heavier arsolyl ligands for the classical divalent lanthanides Yb and Sm but could not obtain their crystal structure and solely characterized them by NMR spectroscopy.[2] Since then, the coordination of various heterocyclic ligands such as dianionic boroles[3,4] and the well-studied group 14 metalloles[5] such as siloles,[6] germoles,[6−8] and plumboles[9] to rare-earth elements has been accomplished (Figure 1). However, among all of the anionic heteroles, phospholyl ligands continue to be the most extensively studied to date.

The study of phospholyl complexes has yielded a wide range of structurally diverse compounds involving both divalent and trivalent lanthanides.[10] For divalent lanthanides, both monomeric and dimeric phospholyl complexes have been obtained.[11−14] A convenient pathway to obtain trivalent lanthanide phospholyl complexes is the oxidation of the divalent ones.[15−18] Additionally, trivalent lanthanide complexes have been obtained through metathesis reactions with the respective halides,[19,20] borohydrides,[21] and alkyls.[22,23] In 2019, the Mills group reported a bis(phospholyl)-dysprosocenium complex,[24] for which a maximum hysteresis temperature of 48 K was achieved. This intriguing discovery showcased the utilization of phospholyl ligands as an alternative axial ligand compared to Cp ligands, challenging the dominance of Cp-based systems in the design of single-molecule magnets (SMMs).[25]

In contrast, examples of complexes with arsolyl ligands remain scarce. After the discovery of the first arsolyl complexes with the classical divalent lanthanides Sm and Yb, Nief and co-workers were able to synthesize the first divalent thulium complexes with arsolyl ligands in 2002.[26] However, to date, there is only one known example of an arsolyl complex with a trivalent lanthanide ion, which was synthesized by a redox reaction between divalent $[Cp^*_2Sm]$ (Cp^* = $C_5Me_5^-$) and a 1,1′-bisarsolyl.[16] However, the resulting compound $[Cp^*_2Sm$-

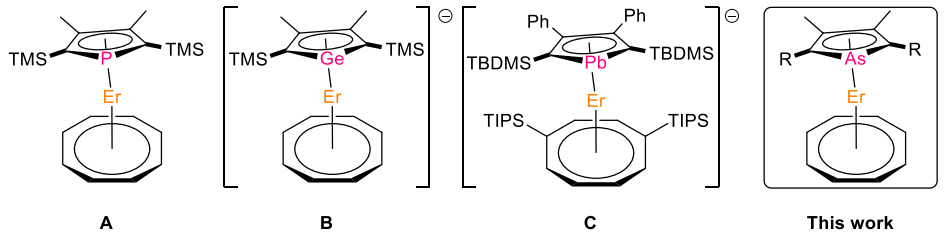

Figure 1. Molecular structures of Er-based SMMs with heterocyclopentadienyl ligands [Er(Dsp)(COT)] (**A**),[28] [Er(L^{Ge})(COT)]$^-$ (**B**),[8] and [Er(L^{Pb})(COT^{TIPS})]$^-$ (**C**).[9] The cations of **B** and **C** are omitted for clarity. Dsp = 3,4-dimethyl-2,5-bis(trimethylsilyl)phospholyl, L^{Ge} = 3,4-dimethyl-2,5-bis(trimethylsilyl)germolyl, L^{Pb} = 3,4-dimethyl-2,5-bis(*tert*-butyldimethylsilyl)plumbolyl, and COT^{TIPS} = 1,4-bis(triisopropylsilyl)-cyclooctatetraendiide.

Scheme 1. Synthesis of the Potassium Arsolyl Complexes 1a, 1b, and 1c

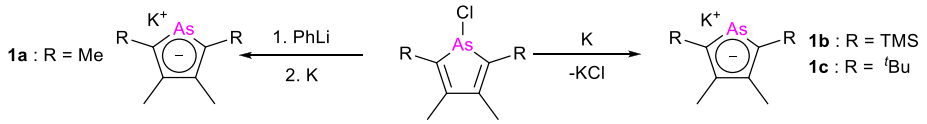

Scheme 2. Synthesis of Samarium Arsolyl Complexes 2-Sm, 3-Sm, and 4-Sm by a Salt Elimination Reaction

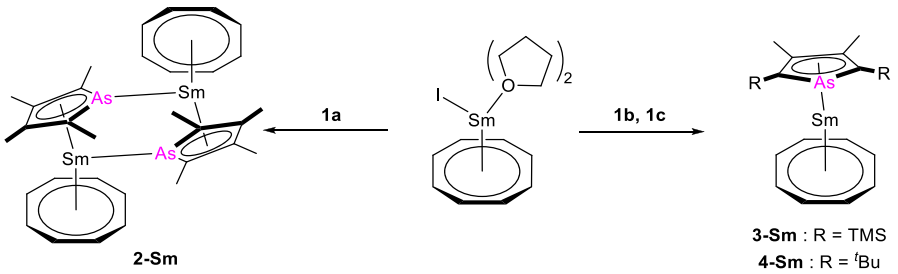

((3,4-dimethylarsolyl))] is not a sandwich complex due to the coordination of three cyclic ligands. In 2015, the first actinide complex incorporating an arsolyl ligand was obtained by the classical metathesis reaction upon reacting UI_3 with a potassium arsolyl complex and K_2COT^{TIPS} (COT^{TIPS} = 1,4-bis(triisopropylsilyl)cyclooctatetraendiide).[27] The dianionic cyclooctatetraendiide ligand has also been used in the synthesis of linear-type lanthanide phospholyl sandwich compounds [Ln(COT)(Dsp)] (Dsp = 3,4-dimethyl-2,5-bis(trimethylsilyl)-phospholyl and COT = η^8-C_8H_8).[28] The erbium compound of this type was of particular interest because it shows enhanced magnetic properties compared to the fully carbon-based [Er(COT)(Cp*)].[29]

These results raise the question of whether it is possible to form similar complexes by using arsolyl ligands with the aim of studying if and how the softer As atom affects the structure and magnetism of the corresponding complexes. Herein, we showcase the synthesis and structural characterization of a series of trivalent lanthanide sandwich complexes ligated by distinct arsolyl and COT ligands. In addition, the magnetic behavior of a selected erbium complex was investigated and compared to those of related known complexes.

RESULTS AND DISCUSSION

For synthesizing the desired arsolyl-functionalized sandwich complexes, we employed three different arsolyl ligands. The potassium salts of two of these arsolyl compounds, **1a**[2] (KTmas, where Tmas = 2,3,4,5-tetramethylarsolyl) and **1b**[26] (KDsas, where Dsas = 3,4-dimethyl-2,5-bis(trimethylsilyl)-arsolyl]) were already described in the literature. In addition, the previously unknown ^{t}Bu-substituted potassium arsolyl complex **1c** (KDtas, where Dtas = 3,4-dimethyl-2,5-bis(*tert*-butyl)arsolyl) was synthesized (Scheme 1).

These potassium arsolyl complexes were then reacted with [Sm(COT)I$(THF)_2$][30] at room temperature in tetrahydrofuran (THF), to give the corresponding sandwich complexes [Sm(COT)$(Tmas)]_2$ (**2-Sm**), [Sm(COT)(Dsas)] (**3-Sm**), and [Sm(COT)(Dtas)] (**4-Sm**) (Scheme 2) after extraction with toluene as an air-sensitive material. Single crystals of all three complexes were obtained in a moderate yield from their concentrated toluene solutions at room temperature.

Single-crystal X-ray diffraction (SCXRD) analysis of complex **2-Sm** revealed a dimeric structure with the formula $[Sm(COT)(Tmas)]_2$, exhibiting a μ:η^5-η^1 coordination mode of the arsolyl ligands (Figure 2). A similar coordination has also been observed for phospholyls and arsolyls in a previous study by Nief and Ricard of [Cp^*_2Sm((3,4-dimethylarsol-yl))].[16] Within the η^5-coordinated sandwich scaffold, the Sm−As bond length is 3.0364(3) Å, while the corresponding η^1 Sm′−As bond, which is bridging the two sandwich units, is about 0.2 Å longer [Sm′−As: 3.2192(3) Å]. As a consequence of this unique coordination mode involving the As atoms, the Ct_{COT}−Sm−Ct_{Tmas} angle becomes significantly bent [146.54(2)°].

In contrast, samarium complexes **3-Sm** and **4-Sm** crystallize as monomeric sandwich structures in the solid state (Figure 2). This led us to conclude that the low steric demand of the two methyl groups in the 2 and 5 positions of the Tmas ligand combined with the size of the Sm ion itself is the reason for the formation of the dimeric structure. A similar observation was found in the neodymium phospholyl complex [(COT)Nd-(Dsp)(THF)], where, due to the larger ionic radius of the Nd

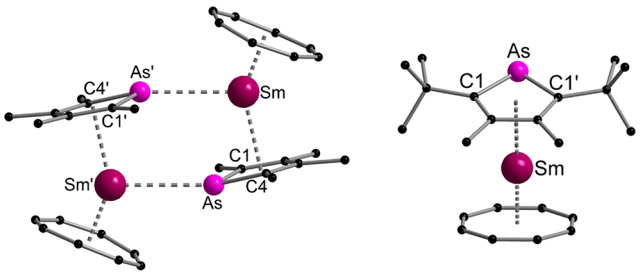

Figure 2. Molecular structures of **2-Sm** (left) and **4-Sm** (right) in the solid state. For better clarity, H atoms are omitted. Selected bond lengths (Å) and angles (deg) for **2-Sm**: Sm−As 3.0364(3), Sm−As′ 3.2192(3), Sm−Ct_{Tmas} 2.5098(3), Sm−Ct_{COT} 1.8730(3); Ct_{Tmas}−Sm−Ct_{COT} 146.54(2). Selected bond lengths (Å) and angles (deg) for **4-Sm**: Sm−As 2.9904(7), Sm−Ct_{Dtas} 2.4636(5), Sm−Ct_{COT} 1.8158(3); Ct_{Dtas}−Sm−Ct_{COT} 164.683(14).

atom, an additional THF molecule is coordinated as an equatorial ligand,[31] which is in contrast to the solvent-free complexes of the smaller lanthanides (Ln = Tb, Dy, Er, Tm).[28] The monomeric samarium complexes also show a more linear structure than dimeric **2-Sm**, as evidenced by the Ct_{COT}−Sm−Ct_{As} angles of 164.24(1)° for **3-Sm** and 164.68(2)° for **4-Sm**. Despite their paramagnetism, these samarium complexes could also be characterized by ^{1}H and ^{13}C{^{1}H} NMR spectroscopy. In the ^{1}H NMR spectrum, the signal of the COT protons is seen at 9.93 ppm for **2-Sm**, 9.58 ppm for **3-Sm**, and 9.36 ppm for **4-Sm**. The signal for the methyl protons at the 3 and 4 positions of the arsolyl ligand is found at 3.73 ppm for **3-Sm**, 3.70 ppm for **4-Sm**, and 3.95 ppm for **2-Sm**.

To further explore the coordination behavior of the arsolyl ligands with smaller lanthanides, our focus turned to dysprosium and erbium, for which the respective phospholyl complexes have already been reported previously.[28] In general, sandwich complexes of these elements, are among the best single molecule magnets (SMMs).[3,24,30,32,33] Employing reaction conditions analogous to those used for synthesizing the samarium complexes, we successfully obtained six new complexes [Dy(COT)(Tmas)] (**2-Dy**), [Dy(COT)(Dsas)] (**3-Dy**), [Dy(COT)(Dtas)] (**4-Dy**), [Er(COT)(Tmas)] (**2-Er**), [Er(COT)(Dsas)] (**3-Er**), and [Er(COT)(Dtas)] (**4-Er**) in moderate yields as air sensitive materials (Scheme 3). These complexes were isolated as yellow (Dy) and orange (Er) single crystals from concentrated toluene solutions, except for **2-Dy**, which was crystallized from a concentrated *n*-pentane solution at −10 °C. Interestingly, all of the reaction products exhibited a monomeric solid-state structure (Figures 3 and 4). This exclusively monomeric behavior can be attributed to the smaller ionic radius of Dy and Er in comparison to Sm.[34] Thermogravimetric analysis of compound **4-Er** was performed to investigate the thermal stability (Figure S41). Compound **4-Er** is stable until about 84 °C and then slowly loses about 3% of it mass upon heating to about 200 °C. Significant weight loss was seen in the range between 315 and 370 °C.

Due to the similarities in the molecular structures, the discussion herein is focused on the three erbium complexes **2-Er**, **3-Er**, and **4-Er** (Figure 3).[34] All trends that will be discussed in the following section were also observed for the dysprosium compounds (Figure 4).

As anticipated, compound **2-Er** exhibits the shortest Er−As distance of 2.8699(5) Å, primarily attributed to the low steric demand of the ligand. In contrast, compounds **3-Er** and **4-Er** display slightly longer Er−As distances of 2.9138(6) and 2.9104(6) Å, respectively, due to the presence of the bulkier tetramethylsilyl and ^{t}Bu groups. A similar trend is observed for the Er−Ct_{As} distances, with **2-Er** having the shortest distance of 2.3297(4) Å, while **3-Er** and **4-Er** exhibit slightly longer distances of 2.3523(4) and 2.3492(3) Å. The Er−Ct_{COT} distance of 1.6774(4) Å in complex **2-Er** is also the shortest among the three compounds, which is comparable to the Er−Ct_{COT} distance in the previously reported [Er(COT)Cp*] complex with 1.662 Å.[29] For **3-Er** and **4-Er**, the Er−Ct_{COT} distances are longer with 1.7051(3) and 1.7001(2) Å.

The bond angles between the centroids of the ligands and the Er atom provide insights into the linearity of the complex. Compound **2-Er** exhibits a Ct_{As}−Er−Ct_{COT} angle of 164.86(2)°, while **3-Er** and **4-Er** display angles of 167.52(2)° and 167.647(12)°, respectively. The tilting angle between the two ligand planes also demonstrates this trend, with **3-Er** and **4-Er** having angles of 15.1° and 15.2°, respectively, while **2-Er** has a larger angle of 17.7°, deviating further from a linear geometry. The shortest intermolecular Er−Er distance in **4-Er** is 7.6071(6) Å, while the shortest intermolecular Dy−Dy distance in **4-Dy** is 7.7243(3) Å, consistent with the bigger ionic radius of Dy compared to Er.

We also compared the arsolyl COT complexes **3-Er** and **4-Er** to the literature-known phosphoyl complex [Er(COT)(Dsp)] and the Cp*-based species [Er(COT)(Cp*)]. Compared to [Er(COT)(Dsp)], compounds **3-Er** and **4-Er** demonstrate slightly longer Er−Ct_{COT} distances of 1.7051(3) and 1.7001(2) Å (compared to 1.686 Å in the phosphorus compound) but slightly shorter than the distance in [Er(COT)Cp*].[29] Furthermore, the Er−Ct_{As} distances measure 2.3523(4) Å for **3-Er** and 2.3492(3) Å for **4-Er**, slightly longer than that of Er−Ct_{Dsp} (2.321 Å), while the Er−As bond lengths of 2.9138(6) and 2.9104(6) Å are longer than the corresponding Er−P bond length of 2.793 Å. In comparison to the erbium phospholyl complex, which has a Ct_{Dsp}−Er−Ct_{COT} angle of 170.8°, erbium complexes **3-Er** and **4-Er** are slightly less linear sandwich complexes.

This distinction is also evident in the tilting angle between the COT and Dsas ligands, measuring 15.1° in **3-Er** and 15.2° in **4-Er**, compared to only 10.5° in [Er(COT)(Dsp)]. This variation in the coordination geometry can be attributed to the larger size of the As atom relative to the P atom as well as the

Scheme 3. Synthesis of Erbium and Dysprosium Arsolyl Complexes 2-Dy, 3-Dy, 4-Dy, 2-Er, 3-Er, and 4-Er

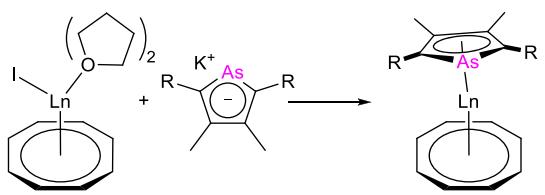

2-Dy : Ln = Dy, R = Me 39%
3-Dy : Ln = Dy, R = TMS 50%
4-Dy : Ln = Dy, R = ^{t}Bu 56%

2-Er : Ln = Er, R = Me 63%
3-Er : Ln = Er, R = TMS 49%
4-Er : Ln = Er, R = ^{t}Bu 58%

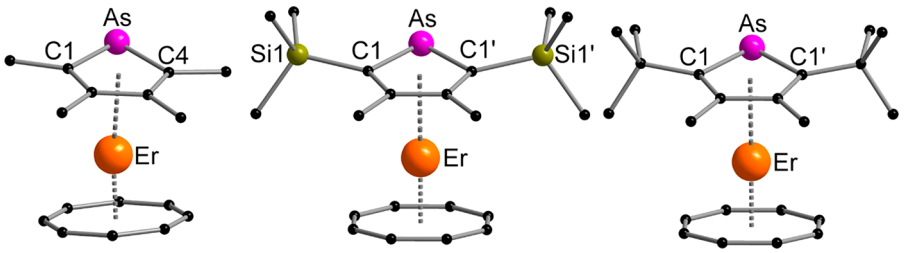

Figure 3. Molecular structures **2-Er** (left), **3-Er** (middle), and **4-Er** (right) in the solid state. For better clarity, hydrogen atoms are omitted. Selected bond lengths (Å) and angles (deg) for **2-Er**: Er–As 2.8699(5), Er–Ct_{Tmas} 2.3297(4), Er–Ct_{COT} 1.6774(4); Ct_{Tmas}–Er–Ct_{COT} 164.86(2). Selected bond lengths (Å) and angles (deg) for **3-Er**: Er–As 2.9138(6), Er–Ct_{Dsas} 2.3523(4), Er–Ct_{COT} 1.7051(3); Ct_{Tmas}–Er–Ct_{COT} 167.52(2). Selected bond lengths (Å) and angles (deg) for **4-Er**: Er–As 2.9104(6), Er–Ct_{Dtas} 2.3492(3), Er–Ct_{COT} 1.7001(2); Ct_{Dtas}–Er–Ct_{COT} 167.647(12).

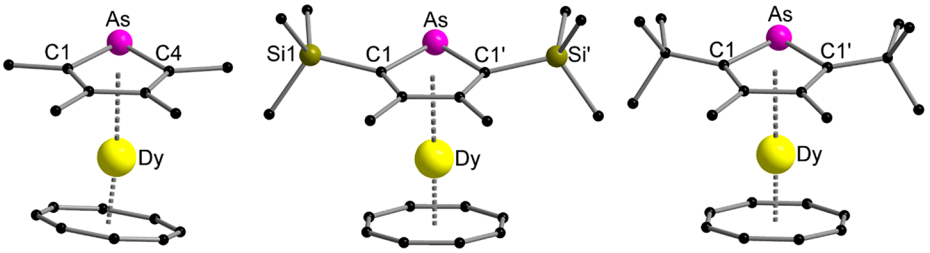

Figure 4. Molecular structures **2-Dy** (left), **3- Dy** (middle), and **4- Dy** (right) in the solid state. For better clarity, hydrogen atoms are omitted. Selected bond lengths (Å) and angles (deg) for **2-Dy**: Dy–As 2.9176(4), Dy–Ct_{Tmas} 2.3800(3), Dy–Ct_{COT} 1.7266(3); Ct_{Tmas}–Er–Ct_{COT} 163.79(2). Selected bond lengths (Å) and angles (deg) for **3-Dy**: Dy–As 2.9450(5), Dy–Ct_{Dsas} 2.3900(2), Dy–Ct_{COT} 1.7385(2); Ct_{Dsas}–Dy–Ct_{COT} 166.526(12). Selected bond lengths (Å) and angles (deg) for **4-Dy**: As–Dy 2.9548(4), Dy–Ct_{Dtas} 2.4037(2), Dy–Ct_{COT} 1.7516(2); Ct_{Dtas}–Dy–Ct_{COT} 167.047(12).

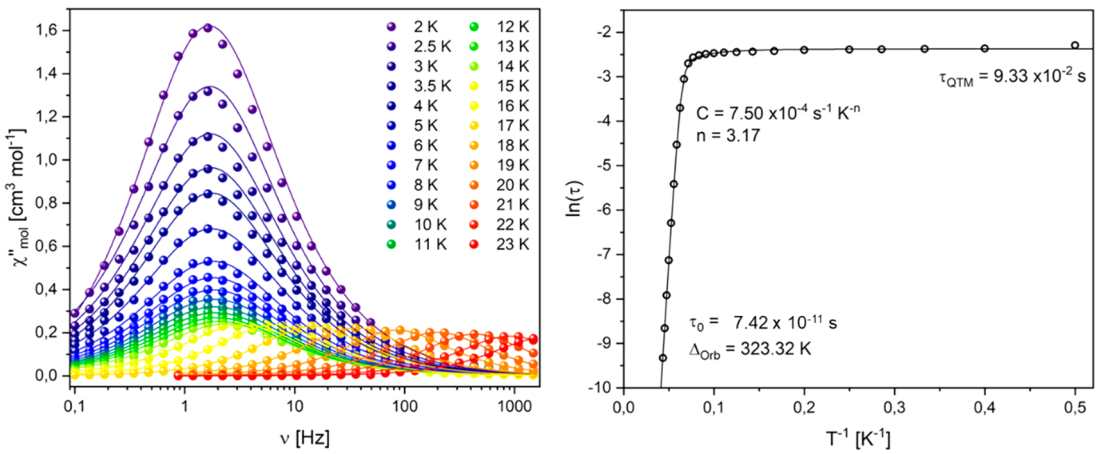

Figure 5. Frequency-dependent out-of-phase susceptibility (left) and Arrhenius plot (right).

weaker coordination between erbium and the arsolyl ligands. Overall, we can anticipate that the softer arsolyl ligand seems to be a weaker axial ligand compared to the lighter phospholyl congener, but simultaneously the equatorial COT ligand in the arsolyl compound is also further away from the Er^{3+} ion than in the phospholyl complex. Because the structures of **3-Er** and **4-Er** are very similar, we decided to perform the following magnetic measurements with **4-Er** because this compound crystallizes better and can also be obtained in higher yields.

MAGNETIC PROPERTIES OF 4-ER

Due to the high anisotropic nature of Ln^{3+} ions from strong spin–orbit coupling, they show SMM behavior. As described by Rinehart and Long, the presence of equatorial ligand fields can stabilize the prolate m_J state, for example, in Er^{3+}.[35] The COT ligand serves as an outstanding example that exhibits a distinct equatorial field. Exploiting this characteristic, we performed an extensive investigation into the magnetic properties of the erbium complex **4-Er**.

The temperature-dependent magnetic behavior of **4-Er** was measured in the 300–2 K range in an external magnetic field of 1000 Oe (0.1 T). Complex **4-Er** showed a molar $\chi_M T$ value at room temperature of 9.77 K. These observed values are around 15% below the expected value of a single isolated Er^{3+} ion of 11.48 cm^3 K mol^{-1}. This might be attributed to the errors that occurred during the sample preparation process, wherein the sample was inadvertently smeared across the glass walls while flame-sealing it in an NMR tube. Upon cooling, $\chi_M T$ slowly decreases below 150 K to about 9.0 cm^3 K mol^{-1} at 5 K. Then an abrupt drop of susceptibility at very low temperatures can

be seen, which indicates magnetic blocking as a result of an anisotropic ion in a strong ligand field. Considering the shortest intermolecular Er−Er distances of 7.6 Å (vide supra), antiferromagnetic coupling between neighboring Er ions could contribute to the observed drop of $\chi_M T$. The molar magnetization versus the applied magnetic field measurements on complex **4-Er** showed a rapid increase in magnetization, which strongly flattens upon reaching higher fields (Figure S29, inset). With values around 4 μ_B mol^{-1} at 7 T, the values are again about 10% below the expected value for a single highly anisotroptic Er^{3+} ion of 4.5 μ_B mol^{-1},[29,30] therefore being in line with the susceptibilities that we observed. At low fields below 0.5 T, a sigmoidal curvature is observed that is a result of the magnetic blocking, allowing alignment of the magnetic moments only at strong applied fields.

We also studied the dynamic behavior of compound **4-Er** with alternating-current susceptibility measurements. The studies show a frequency-dependent out-of-phase component of magnetic susceptibility in a zero direct-current field. In the temperature region of 2−12 K, the maximum is almost constant around 2 Hz, which describes the temperature-independent region, where relaxation occurs via quantum tunneling of magnetization (QTM). On the other hand, the frequency shifts to higher values with increasing temperature (Figure 5) from 12 to 23 K are typically associated with an Orbach process of relaxation in SMMs. By fitting the in-phase and out-of-phase signals using a generalized Debye model, we obtained the parameter α between 0.18 at lower temperature and 0.003 at higher temperature (Table S4). This suggests that at lower temperatures other processes like Raman could have been involved, whereas at higher temperatures, the Orbach process is the dominant one. Following this assumption, we performed fits of the temperature-dependent relaxation times using a combination of Orbach, Raman, and QTM relaxation with the equation:

$$\tau^{-1} = \tau_0^{-1} \exp\left(-\frac{\Delta_{Orb}}{k_B T}\right) + CT^n + \tau_{QTM}^{-1}$$

We have found a rather small contribution of the Raman process (with $C = 7.5 \times 10^{-4}$ s^{-1} K^{-n} and $n = 3.17$) and $\tau_{QTM} = 9.33 \times 10^{-2}$ s. On the other hand, the higher temperature analysis gives an energy barrier of $\Delta_{Orb} = 323.32$ K and $\tau_0 = 7.42 \times 10^{-11}$ s.

We performed hysteresis measurements in the range of −2 to +2 T at different temperatures with field sweep rates of 25 and 100 Oe/s (Figures S32 and S33). At 2 K, we observed a butterfly-like hysteresis, open at zero field, at both slower and faster sweep rates of 25 and 100 Oe/s, respectively. The butterfly-like shape of the hysteresis is typical for lanthanide ions, where the abrupt drops are caused by efficient QTM at fields close to zero. Under faster sweep rates, hysteresis can be observed until 10 K (Figures S32−S35). Extrapolation of the Orbach relaxation data gives the calculated temperature of $T = 11.5$ K, where $\tau = 100$ s,[36,37] which is in decent agreement with the hysteresis loop observed.

To verify the experimental values, we performed ab initio complete active space self-consistent-field (CASSCF) calculations using the *MOLCAS* package, and the simulated $\chi_M T$ vs T behavior of **4-Er** is in good agreement after a small scaling factor of 0.9 is applied. The deviation observed in the very low temperature region is due to magnetic blocking, as previously stated. The calculation of the low-lying Kramer's doublet shows pure $m_J = |^{15}/_2\rangle$ states to be the ground states characterized by $g_x < g_y < 0.001$ and $g_z = 17.91$, suggesting highly axial ground states as a result of the equatorial ligand field.[38] The low transverse component of the **g** tensor gives a low probability for QTM, which is in good agreement with the observation of the SMM behavior at zero field. Analysis of the calculated transition probabilities suggests that the most likely relaxation pathway occurs through the fourth excited state, which is calculated at 329 K (Figure S36) and is in very good agreement with the experimentally observed energy barrier.

The energy barrier of complex **4-Er** (U_{eff} = 323.3 K) is slightly smaller compared to the previously reported [Er(COT)(Dsp)] complex (U_{eff} = 358 K), even with slight structural differences in the Er-COT distance of 1.7001(2) Å in **4-Er** (1.6855 Å in [(Dsp)Er(COT)]) and a tilting angle of the planes of 15.2° for **4-Er** (10.5° for (Dsp)Er(COT)). On the other hand, upon comparison to [(Cp*)Er(COT)], **4-Er** shows a very similar energy barrier. Compared to the reported complex [(Cp^{ttt})Er(COT)] with an energy barrier of 328 K, the arsolyl complex **4-Er** shows a slightly worse barrier. Therefore, introducing a softer atom like As has shown slightly worse properties compared to that of the phospholyl complex but has shown similar magnetic dynamics compared to the parent complex [(Cp*)Er(COT)].

We have performed a similar magnetic analysis for **4-Dy** (Figures S37−S41 and Tables S6 and S7). Due to the intrinsic anisotropy, Dy-SMMs benefit from an axial ligand field, opposite to that of the erbium compounds. The equatorial ligand field in **4-Ln** is, therefore, nonbeneficial for Dy. We have found **4-Dy** to be a field-induced SMM with an energy barrier of U_{eff} = 78.6 K at an optimal field of 600 Oe. At zero field, slow relaxation is quenched due to efficient QTM. Ab initio calculations suggest that the relaxation of **4-Dy** occurs via the second excited state (Figure S42).

CONCLUSION

In summary, we employed two preexisting potassium arsolyl complexes alongside a newly synthesized variant to create a range of lanthanide arsolyl complexes featuring cyclooctatetraendiide ligands. This resulted in the classical sandwich complexes [(η^5-C_4R_4As)Ln(η^8-C_8H_8)], with the exception of one dimeric samarium complex, which can be rationalized due to the relatively low steric demand of the tetramethyl-substituted arsolyl ligand coupled with the larger ionic radius of the Sm ion compared to Dy and Er, resulting in an interesting μ;η^5-η^1 coordination mode of the As atoms. Additionally, despite their paramagnetism, the samarium complexes could be characterized by NMR spectroscopy. To showcase the SMM behavior of the heavier congeners, we conducted an in-depth magnetic analysis on two of the complexes. The erbium analogue revealed hysteresis up to 11.5 K and an energy barrier of U_{eff} = 323.3 K. To complement these experimental findings, ab initio CASSCF calculations were also performed.

Considering magnetic properties similar to those of the existing erbium complexes featuring cyclopentadienyl ligands, our work underscores the potential of arsolyl ligands in SMM design. This study not only expands the limited class of trivalent lanthanide arsolyl complexes but also contributes to the broader exploration of these ligands for future applications.

AUTHOR INFORMATION

Corresponding Author

Peter W. Roesky − *Institute of Inorganic Chemistry, Karlsruhe Institute of Technology, 76131 Karlsruhe, Germany;* orcid.org/0000-0002-0915-3893; Email: roesky@kit.edu

Authors

Noah Schwarz − *Institute of Inorganic Chemistry, Karlsruhe Institute of Technology, 76131 Karlsruhe, Germany*

Frederic Krätschmer − *Institute of Inorganic Chemistry, Karlsruhe Institute of Technology, 76131 Karlsruhe, Germany*

Nithin Suryadevara − *Institute for Quantum Materials and Technologies, Karlsruhe Institute of Technology, D-76344 Eggenstein-Leopoldshafen, Germany;* orcid.org/0000-0002-8193-3878

Sören Schlittenhardt − *Institute of Nanotechnology, Karlsruhe Institute of Technology, D-76344 Eggenstein-Leopoldshafen, Germany*

Mario Ruben − *Institute for Quantum Materials and Technologies and Institute of Nanotechnology, Karlsruhe Institute of Technology, D-76344 Eggenstein-Leopoldshafen, Germany; Centre Européen de Science Quantique, Institut de Science et d'Ingénierie Supramoléculaires, Université de Strasbourg, 67083 Strasbourg Cedex, France*

Author Contributions

†Both authors contributed equally.

Author Contributions

N.S. and F.K. synthesized and analyzed all compounds. N.S. and S.S. conducted the magnetic measurements and calculations and interpreted the results. P.W.R. originated the idea, supervised the work, and interpreted the results. All authors contributed to the preparation of the manuscript. All authors have given approval to the final version of the manuscript.

Funding

This work is supported by the German Federal Ministry of Education and Research (BMBF) under Contract 02NUK059F. Deutsche Forschungsgemeinschaft is acknowl-edged for financial support within the Reinhart Koselleck-Projekt 440644676, RO 2008/19-1 and the Collaborative Research Centre "4f for Future" (CRC 1573 project number 471424360, projects B1 and B3).

Notes

The authors declare no competing financial interest.

ACKNOWLEDGMENTS

We are grateful to Maxime Bonnin for performing thermogravimetric analysis of **4-Er**.

REFERENCES

(1) Nief, F.; Mathey, F. A new application of the tetramethylphospholyl (η^5-C_4Me_4P) π-ligand. Synthesis of η^5-tetramethylphospholyl complexes of yttrium and lutetium. *J. Chem. Soc., Chem. Commun.* **1989**, 800−801.

(2) Nief, F.; Ricard, L.; Mathey, F. Phospholyl (phosphacyclopentadienyl) and arsolyl (arsacyclopentadienyl) complexes of ytterbium(II) and samarium(II). Synthetic, structural and multinuclear (^{31}P and ^{171}Yb) NMR studies. *Polyhedron* **1993**, *12*, 19−26.

(3) Vanjak, J. C.; Wilkins, B. O.; Vieru, V.; Bhuvanesh, N. S.; Reibenspies, J. H.; Martin, C. D.; Chibotaru, L. F.; Nippe, M. A High-Performance Single-Molecule Magnet Utilizing Dianionic Aminoborolide Ligands. *J. Am. Chem. Soc.* **2022**, *144*, 17743−17747.

(4) Zhu, D.; Wang, M.; Guo, L.; Shi, W.; Li, J.; Cui, C. Synthesis, Structure, and Magnetic Properties of Rare-Earth Benzoborole Complexes. *Organometallics* **2021**, *40*, 2394−2399.

(5) Sun, X.; Roesky, P. W. Group 14 metallole dianions as η^5-coordinating ligands. *Inorg. Chem. Front.* **2023**, *10*, 5509−5516.

(6) Sun, X.; Münzfeld, L.; Jin, D.; Hauser, A.; Roesky, P. W. Silole and germole complexes of lanthanum and cerium. *Chem. Commun.* **2022**, *58*, 7976−7979.

(7) Liu, J.; Singh, K.; Dutta, S.; Feng, Z.; Koley, D.; Tan, G.; Wang, X. Yttrium germole dianion complexes with Y-Ge bonds. *Dalton Trans.* **2021**, *50*, 5552−5556.

(8) De, S.; Mondal, A.; Ruan, Z.-Y.; Tong, M.-L.; Layfield, R. A. Dynamic Magnetic Properties of Germole-ligated Lanthanide Sandwich Complexes. *Chem. Eur. J.* **2023**, *29*, No. e202300567.

(9) Münzfeld, L.; Sun, X.; Schlittenhardt, S.; Schoo, C.; Hauser, A.; Gillhuber, S.; Weigend, F.; Ruben, M.; Roesky, P. W. Introduction of plumbole to f-element chemistry. *Chem. Sci.* **2022**, *13*, 945−954.

(10) Mills, D. P.; Evans, P. f-Block Phospholyl and Arsolyl Chemistry. *Chem. Eur. J.* **2021**, *27*, 6645−6665.

(11) Jaroschik, F.; Nief, F.; Le Goff, X.-F.; Ricard, L. Synthesis and Reactivity of Organometallic Complexes of Divalent Thulium with Cyclopentadienyl and Phospholyl Ligands. *Organometallics* **2007**, *26*, 3552−3558.

(12) Nief, F.; de Borms, B. T.; Ricard, L.; Carmichael, D. New Complexes of Divalent Thulium with Substituted Phospholyl and Cyclopentadienyl Ligands. *Eur. J. Inorg. Chem.* **2005**, *2005*, 637−643.

(13) Nief, F.; Ricard, L. Synthesis of η^1 and η^5 complexes of samarium(II) with benzophospholyl ligands. *J. Organomet. Chem.* **1994**, *464*, 149−154.

(14) Nief, F.; Ricard, L. Phosphorus−heteroatom bond cleavage by ytterbium metal. Synthesis of mono(η^5-tetramethylphospholyl)-ytterbium(II) chloride and thiolate complexes and structural characterisation of $[Yb(\mu\text{-}Cl)(\eta^5\text{-}C_4Me_4P)(thf)_2]_2$ and $[Yb(\mu\text{-}SPh)(\eta^5\text{-}C_4Me_4P)(thf)_2]_2$. *J. Chem. Soc., Chem. Commun.* **1994**, 2723−2724.

(15) Barbier-Baudry, D.; Heiner, S.; Kubicki, M. M.; Vigier, E.; Visseaux, M.; Hafid, A. An Easy Synthetic Route to Heteroleptic Samarium Monoalkoxides for Ring-Opening Polymerization Initiators. Molecular Structures of $[(C_5H^iPr_4)SmI(THF)_2]_2$, $SmI_2O^tBu(THF)_4$, and $(C_4Me_4P)_2SmO^tBu(THF)$. *Organometallics* **2001**, *20*, 4207−4210.

(16) Nief, F.; Ricard, L. Synthesis and Molecular Structure of Bis(pentamethylcyclopentadienyl) Phospholyl- and Arsolylsamarium(III) Complexes: Influence of Steric and Electronic Factors. *Organometallics* **2001**, *20*, 3884−3890.

(17) Jacquot, L.; Xémard, M.; Clavaguéra, C.; Nocton, G. Multiple One-Electron Transfers in Bipyridine Complexes of Bis(phospholyl) Thulium. *Organometallics* **2014**, *33*, 4100−4106.
(18) Jaroschik, F.; Momin, A.; Martinez, A.; Harakat, D.; Ricard, L.; Le Goff, X. F.; Nocton, G. Synthesis and Characterization of 1,1′-Diphosphaplumbocenes: Oxidative Ligand Transfer Reactions with Divalent Thulium Complexes. *Organometallics* **2016**, *35*, 2032−2038.
(19) Jaroschik, F.; Shima, T.; Li, X.; Mori, K.; Ricard, L.; Le Goff, X.-F.; Nief, F.; Hou, Z. Synthesis, Characterization, and Reactivity of Mono(phospholyl)lanthanoid(III) Bis(dimethylaminobenzyl) Complexes. *Organometallics* **2007**, *26*, 5654−5660.
(20) Jaroschik, F.; Nief, F.; Le Goff, X.-F. Sterically hindered cyclopentadienyl and phospholyl ligands in dysprosium chemistry. *Polyhedron* **2009**, *28*, 2744−2748.
(21) Cendrowski-Guillaume, S. M.; Le Gland, G.; Nierlich, M.; Ephritikhine, M. Lanthanide Borohydrides as Precursors to Organometallic Compounds. Mono(cyclooctatetraenyl) Neodymium Complexes. *Organometallics* **2000**, *19*, 5654−5660.
(22) Le Roux, E.; Nief, F.; Jaroschik, F.; Törnroos, K. W.; Anwander, R. Mono-phosphacyclopentadienyl bis(tetramethylaluminate) lanthanide complexes. *Dalton Trans.* **2007**, 4866−4870.
(23) Le Roux, E.; Liang, Y.; Törnroos, K. W.; Nief, F.; Anwander, R. Heterogenization of Lanthanum and Neodymium Monophosphacyclopentadienyl Bis(tetramethylaluminate) Complexes onto Periodic Mesoporous Silica SBA-15. *Organometallics* **2012**, *31*, 6526−6537.
(24) Evans, P.; Reta, D.; Whitehead, G. F. S.; Chilton, N. F.; Mills, D. P. Bis-Monophospholyl Dysprosium Cation Showing Magnetic Hysteresis at 48 K. *J. Am. Chem. Soc.* **2019**, *141*, 19935−19940.
(25) Goodwin, C. A. P. Blocking like it's hot: a synthetic chemists' path to high-temperature lanthanide single molecule magnets. *Dalton Trans.* **2020**, *49*, 14320−14337.
(26) Nief, F.; Turcitu, D.; Ricard, L. Synthesis and structure of phospholyl- and arsolylthulium(II) complexes. *Chem. Commun.* **2002**, 1646−1647.
(27) Kahan, R. J.; Cloke, F. G. N.; Roe, S. M.; Nief, F. Activation of carbon dioxide by new mixed sandwich uranium(III) complexes incorporating cyclooctatetraenyl and pyrrolide, phospholide, or arsolide ligands. *New J. Chem.* **2015**, *39*, 7602−7607.
(28) Chen, S.-M.; Xiong, J.; Zhang, Y.-Q.; Yuan, Q.; Wang, B.-W.; Gao, S. A soft phosphorus atom to "harden" an erbium(III) single-ion magnet. *Chem. Sci.* **2018**, *9*, 7540−7545.
(29) Jiang, S.-D.; Wang, B.-W.; Sun, H.-L.; Wang, Z.-M.; Gao, S. An organometallic single-ion magnet. *J. Am. Chem. Soc.* **2011**, *133*, 4730−4733.
(30) Münzfeld, L.; Schoo, C.; Bestgen, S.; Moreno-Pineda, E.; Köppe, R.; Ruben, M.; Roesky, P. W. Synthesis, structures and magnetic properties of $[(\eta^9\text{-}C_9H_9)Ln(\eta^8\text{-}C_8H_8)]$ super sandwich complexes. *Nat. Commun.* **2019**, *10*, 3135.
(31) Visseaux, M.; Nief, F.; Ricard, L. Synthesis of mixed phospholyl/cyclooctatetraenyl−lanthanide complexes. Crystal and molecular structure of (cyclooctatetraenyl)[3,4-dimethyl-2,5-bis-(trimethylsilyl)-phospholyl](tetrahydrofuran)neodymium. *J. Organomet. Chem.* **2002**, *647*, 139−144.
(32) Guo, F.-S.; Day, B. M.; Chen, Y.-C.; Tong, M.-L.; Mansikkamäki, A.; Layfield, R. A. Magnetic hysteresis up to 80 K in a dysprosium metallocene single-molecule magnet. *Science* **2018**, *362*, 1400−1403.
(33) Goodwin, C. A. P.; Ortu, F.; Reta, D.; Chilton, N. F.; Mills, D. P. Molecular magnetic hysteresis at 60 K in dysprosocenium. *Nature* **2017**, *548*, 439−442.
(34) Shannon, R. D. Revised effective ionic radii and systematic studies of interatomic distances in halides and chalcogenides. *Acta Crystallogr., Sect. A* **1976**, *32*, 751−767.
(35) Rinehart, J. D.; Long, J. R. Exploiting single-ion anisotropy in the design of f-element single-molecule magnets. *Chem. Sci.* **2011**, *2*, 2078−2085.
(36) Le Roy, J. J.; Ungur, L.; Korobkov, I.; Chibotaru, L. F.; Murugesu, M. Coupling Strategies to Enhance Single-Molecule Magnet Properties of Erbium−Cyclooctatetraenyl Complexes. *J. Am. Chem. Soc.* **2014**, *136*, 8003−8010.
(37) Woodruff, D. N.; Winpenny, R. E. P.; Layfield, R. A. Lanthanide Single-Molecule Magnets. *Chem. Rev.* **2013**, *113*, 5110−5148.
(38) Liddle, S. T.; van Slageren, J. Improving f-element single molecule magnets. *Chem. Soc. Rev.* **2015**, *44*, 6655−6669.